

Synchronization Stability Analysis of Fractional-Order Virtual Synchronous Converter

Bingnan Zhou
Nanjing Normal University
Nanjing China
15075083890@163.com

Zhenyu Lv
Nanjing Normal University
Nanjing China
lvzhenyumath@yeah.net

Qi Li
Nanjing Normal University
Nanjing China
1652030115@qq.com

Cheng Mei
Nanjing Normal University
Nanjing China
736369174@qq.com

Abstract—The traditional virtual synchronous generator(VSG)control strategy provides virtual damping and inertia for the inverter in grid-connected operation, thereby enhancing the frequency and voltage support capability of the system. Nevertheless, the incorporation of virtual inertia will elevate the order of the system, engendering an oscillation in the output active power during the grid-connected operation of the inverter. Furthermore, the virtual inertia and damping will impede the responsiveness of the system. In light of the aforementioned analysis of the frequency domain characteristics of the fractional-order virtual inertia link, this paper puts forth a fractional-order virtual inertia virtual synchronous generator control strategy. Furthermore, the control strategy is employed to examine the equal area rule with fractional order, utilising the fault limit clearing time angle as a metric to assess the system's margin for large disturbance (transient) synchronisation. Additionally, the influencing factors of VSG transient synchronisation stability are investigated. The transient synchronisation stability of a fractional-order VSG system is investigated through the implementation of the proposed control strategy, with the simulation results corroborating the enhanced transient synchronous stability afforded by the strategy.

Keywords—fractional-order, virtual synchronous converter, equal area criterion, synchronization stability analysis

I. INTRODUCTION

In the context of the "double carbon" initiative, new energy power generation technology is developing at a rapid pace. New energy units, exemplified by wind power and photovoltaic, are connected to the power grid subsequent to power conversion through power electronic equipment^[1-2]. The control strategy of the power electronic converter can be classified into two categories: grid-following^[3] and grid-building^[4]. These strategies are applicable to diverse scenarios and offer distinct advantages. In grid-following control, the phase of the power grid is tracked by a phase-locked loop, thereby ensuring synchronisation. New energy units typically operate in maximum power point tracking (MPPT)^[5] mode, which lacks both active support and island operation capabilities. An increase in the number of access points will result in a reduction in the inertia level of the power grid, which may have an adverse impact on the safe and stable operation of the power grid. The grid structure control system proactively generates voltage amplitude and phase reference values through outer loop control, thereby providing support for voltage and frequency. This makes it particularly well-suited to island operation mode.

A virtual synchronous generator (VSG)^[6-7] provides inertia support for the system by simulating the rotor motion equation of a synchronous generator, which belongs to a category of grid-connected control. Nevertheless, the virtual inertia introduced by VSG technology increases the order of the system, thereby rendering the output active power of the inverter susceptible to oscillation when connected to the grid. Firstly, the instantaneous anti-interference and overload capacity of VSG is inadequate, resulting in the triggering of a grid-connected inverter protection shutdown due to the current shock caused by long-term power oscillation. Furthermore, the incorporation of virtual inertia and damping results in a reduction in the system's response speed^[8]. In order to address the issue of power oscillation or frequency stability, several researchers have proposed a synchronous generator control strategy based on adaptive virtual inertia or damping^[9-13]. These methods simulate the behaviour of synchronous generators, construct the relationship between frequency or power change rate and virtual inertia, and adaptively change the inertia or damping parameters of VSG control, thereby enhancing the anti-interference capability and overload resilience of the microgrid system. The aforementioned literature enhances the system's performance by modifying the inertial or damping parameters. However, it fails to address the inherent contradiction between the dynamic, steady-state performance, and parameter adjustment of the output active power when the inverter is connected to the grid^[14].

The increasing application of fractional order controllers in power electronics technology is a consequence of their superior performance, which is evidenced by the enhanced control capabilities they afford^[15]. In 1999, Igor Podlubny put forth a proposal for a fractional-order PI λ Du controller. In recent years, fractional-order controllers have demonstrated efficacy in a multitude of fields. Reference[16], a fuzzy fractional order PI λ Du controller is proposed by combining fuzzy control with fractional order PI λ Du. This approach improves the real-time performance and anti-interference of the control system, and can also enhance the steady-state performance of the system. Reference[17], an optimal passive fractional order PID (PFOPID) was designed for grid-connected photovoltaic inverters. The performance of the PFOPID control was then compared with that of conventional PID control, FOPID control and passivity-based control (PBC). It is highlighted that PFOPID is capable of achieving maximum power tracking under a range of operational scenarios and exhibits favourable dynamic characteristics. Reference[18], a novel control scheme combining fractional order control with a virtual synchronous generator is proposed, which effectively achieves damping

power control without oscillation. Reference[19], in light of the frequency domain characteristics of the fractional-order virtual inertia link, a fractional-order virtual inertia virtual synchronous generator control strategy is put forth with the aim of suppressing the oscillation of active power.

This paper presents a study of the synchronous stability analysis method of a virtual synchronous generator (VSG) under large disturbances, with the proposal of a fractional order VSG control strategy. The impact of various factors on the transient synchronous stability of a VSG is examined by utilising the fault limit clearing angle as a metric to assess the margin of stability (in transient conditions) of the system. This paper proposes a method for studying the transient synchronous stability of a fractional-order VSG system. The simulation results demonstrate the efficacy of the proposed control strategy in enhancing transient synchronous stability.

II. MODELLING ANALYSIS

A. A Comparison of the Traditional VSG Circuit Topology and Control Structure

In this paper, the voltage source virtual synchronous generator control structure is adopted as the basis for analysis. Figure 1 illustrates the VSG circuit topology and control structure. The principal circuit is a three-phase DC-AC, which is furnished with an inductance-capacitance LC filter at the outlet of the inverter with the objective of eliminating harmonics in the current. The filter inductor is designated as L_f , the filter capacitor is designated as C_f , the parasitic resistance of the filter inductor is designated as R_{lf} , and the parasitic resistance of the filter capacitor is designated as R_{cf} . Following the filtering process, the circuit is connected to the common bus through the line impedance designated as Z_g .

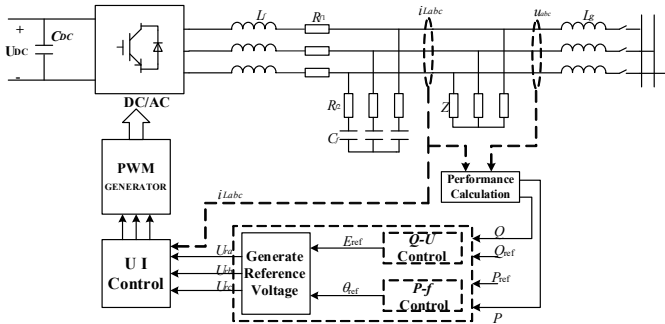


Fig. 1. VSG control structure block diagram

The control section of the VSG is primarily comprised of three distinct components: reactive voltage control, active frequency outer loop control, and voltage and current inner loop control, along with the PWM generator. The control flow is as follows: initially, the voltage and current at the port of the LC filter are collected, and the active and reactive power of the VSG output are calculated. In accordance with the output power, the outer loop generates the voltage loop reference voltage amplitude and phase through the control algorithm. Subsequently, the voltage loop generates the current reference value of the current inner loop through the PI controller, in accordance with the deviation between the voltage reference value and the actual value. The current inner loop then generates

the PWM modulation signal through the PI controller. Subsequently, power conversion is achieved through the implementation of PWM control.

The control component of VSG is primarily subdivided into two distinct categories: outer loop control and inner loop control. The outer loop control comprises two distinct loops: the active control loop and the reactive control loop. The strategy employed for the outer loop control is illustrated in Figure 2.

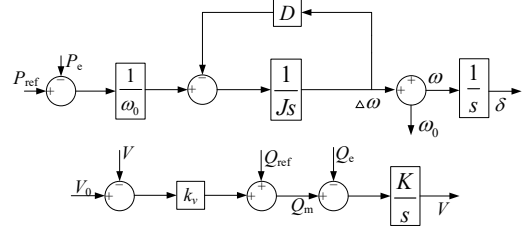


Fig. 2. VSG outer loop control strategy

Figure 2 illustrates that the VSG active power control loop emulates the synchronous generator rotor motion equation, thereby endowing the converter with virtual inertia, virtual damping and primary frequency modulation characteristics. The VSG port voltage reference phase angle δ is then output as the coordinate transformation angle. The reactive power control loop simulates the droop characteristics of reactive power and voltage, and adjusts the reference value of port voltage V in accordance with the output reactive power.

In accordance with the VSG power outer loop control strategy illustrated in Fig. 2, the mathematical models are presented in Equations (1) and (2).

$$\begin{cases} \frac{d\delta}{dt} = \omega - \omega_0 \\ J \frac{d\omega}{dt} = \frac{P_{ref} - P_e}{\omega_0} - D(\omega - \omega_0) \end{cases} \quad (1)$$

$$K \frac{dV}{dt} = Q_{ref} - Q_e - k_v(V - V_0) \quad (2)$$

In the formula, the following variables are defined: J is virtual inertia; D is virtual damping; P_{ref} and P_e are reference active power and output active power, respectively; ω and ω_0 are VSG angular frequency and reference angular frequency, respectively; k_v is the reactive power droop coefficient; K is the voltage loop integral coefficient; Q_{ref} and Q_e are reference reactive power and output reactive power, respectively. V_0 represents the rated output voltage. In order to enhance the precision of control, the VSG control loop is typically equipped with a voltage outer loop and a current inner loop control module. This configuration aligns with the conventional grid-connected converter voltage and current loop control approach. Given that the VSG active outer loop is designed to simulate the rotor motion equation of the synchronous generator, the response speed is relatively slow and the bandwidth is limited. In order to achieve rapid tracking of reference instructions, the bandwidth of the voltage and current loop is significantly larger than that of the active outer loop. Consequently, under the VSG transient synchronous stability time scale, the voltage and current inner

loop response can be considered to have reached a steady state. The influence of the voltage and current loop can be disregarded in the transient synchronous stability analysis of VSG, and the voltage and current inner loop control strategy is no longer described here.

B. Fractional-order VSG Control Strategy

In order to enhance the dynamic performance of the conventional VSG control system and mitigate the power oscillation during the dynamic process, a fractional-order VSG control strategy is put forth in this paper. The power loop control strategy is illustrated in Fig. 3.

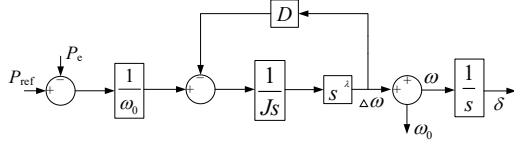


Fig. 3. Fractional-order VSG power loop control strategy

In comparison with the conventional VSG power loop, the integral factor λ is augmented. Subsequently, the fractional-order VSG active power control loop simulates the SG rotor motion equation, which can be expressed as follows:

$$J \frac{d^{1-\lambda} \Delta \omega}{dt^{1-\lambda}} = P_{\text{ref}} - P_e - D(\omega - \omega_0) \quad (3)$$

It is assumed that the phase angle of the grid-side voltage is 0 rad, that the angle δ is identical to the phase angle of the active loop of the fractional-order VSG, and that the closed-loop transfer function of the output electromagnetic power is:

$$P_e = \frac{K_p}{Js^{2-\lambda} + Ds + K_p} P_{\text{ref}} \quad (4)$$

In the formula, K_p represents the gain of the voltage phase angle difference between the two ends of the line δ and the output active power.

As evidenced in Reference[8], the incorporation of virtual inertia into the conventional VSG control strategy results in an elevated order of the system, which in turn gives rise to a reduction in the system's response speed and the emergence of power oscillations. Accordingly, the system order should not exceed that of a second-order system in the design. In this paper, the range of λ is limited to $0 < \lambda < 1$.

The values of J and D are fixed, while the fractional order, represented by λ , is varied. In accordance with Eq. (4), the open-loop Bode diagram of the fractional order virtual inertia VSG control strategy, as illustrated in Fig. 4, is derived.

An examination of the open-loop Bode diagram in Figure 4 reveals that the system employs a fractional-order virtual inertia VSG control strategy, which results in a deceleration of the amplitude attenuation of the middle and high frequency bands of the open-loop system and a reduction in phase lag. The relationship between the open-loop frequency characteristics and the dynamic performance of the closed-loop system demonstrates that the closed-loop system will exhibit reduced

overshoot and rise time, a faster system response, and a notable enhancement in dynamic performance and stability.

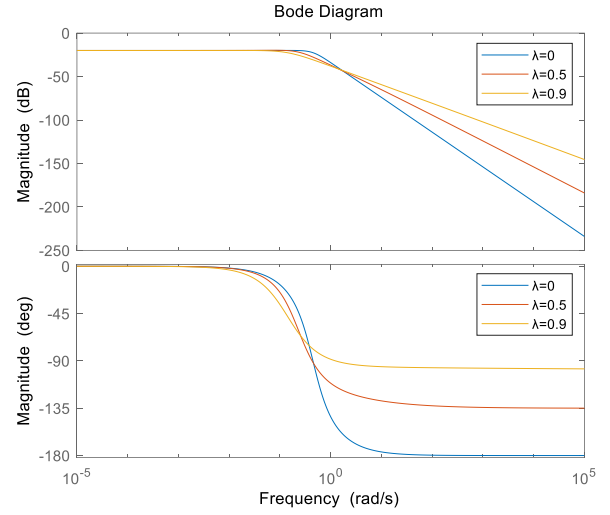


Fig. 4. The open-loop Bode diagram of the fractional-order virtual inertia VSG control strategy and the first-order virtual inertia VSG control strategy

C. Equal Area Rule Considering Fractional Order

This section employs the VSG single-machine infinite-bus system as a case study to examine the operation of the equal area rule in the presence of damping. The configuration of the fractional-order VSG single-machine infinite-bus system is illustrated in Fig. 5.

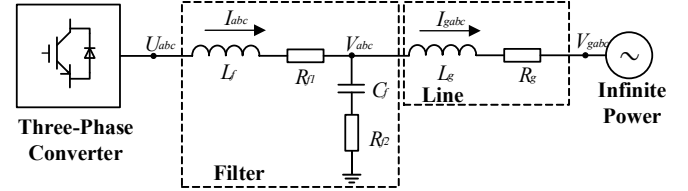


Fig. 5. Fractional order VSG single machine infinite bus system topology

In accordance with the VSG single-machine infinite bus system illustrated in Fig. 5, the output power is demonstrated in Equation (5), with the influence of the line impedance angle excluded.

$$\begin{cases} P = \frac{3}{2} \cdot \frac{V_g V \sin \delta}{X_g} \\ Q = \frac{3}{2} \cdot \frac{V^2 - V_g V \cos \delta}{X_g} \end{cases} \quad (5)$$

In the formula, $X_g = \omega_0 L_g$, V_g represents the phase voltage amplitude of an infinite power supply. V denotes the phase voltage amplitude of the grid-connected point, while δ signifies the phase angle difference between V_g and V . This can be understood as the power angle of a fractional-order VSG single-machine grid-connected system.

This section presents an analysis of the synchronisation stability of the system, taking into account the impact of

damping. The analysis is conducted under the condition of grid-side voltage drop in a fractional-order VSG single-machine infinite-bus system, and the extreme value of the power angle characteristic curve during a fault is less than the reference power. Fig. 6 illustrates the power-angle characteristic curve of the system.

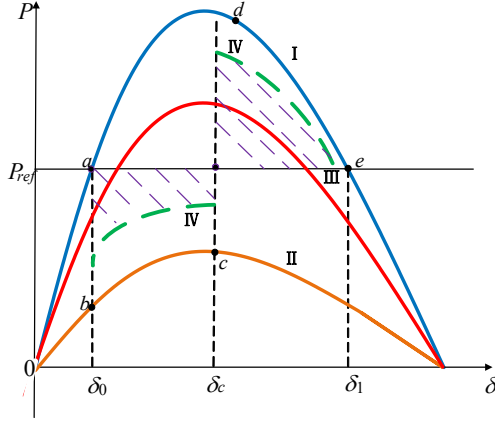


Fig. 6. Equal area rule considering fractional order

In the event of a fault, the rotor motion equation for a VSG single-machine infinite-bus system can be expressed as follows:

$$\dot{\delta} = \omega_1 - \omega_0 = \Delta\omega \quad (6)$$

$$J\omega_0 \dot{\Delta\omega} = P_{\text{ref}} - P_{\text{ef}} - D\omega_0 \Delta\omega \quad (7)$$

The combined formula (6) and formula (7) can be derived as follows:

$$(J\omega_0 \Delta\omega) d^{1-\lambda} \Delta\omega = (P_{\text{ref}} - P_{\text{ef}} - D\omega_0 \Delta\omega) d\delta^{1-\lambda} \quad (8)$$

Where λ is the above integral factor, where $0 < \lambda < 1$.

The integrals of $\Delta\omega$ and δ on both sides of the equation can be obtained as follows:

$$\int_{\Delta\omega_0}^{\Delta\omega_c} (J\omega_0 \Delta\omega) d^{1-\lambda} \Delta\omega = \int_{\delta_0}^{\delta_c} (P_{\text{ref}} - P_{\text{ef}} - D\omega_0 \Delta\omega) d\delta^{1-\lambda} \quad (9)$$

The acceleration and deceleration area of the fractional-order VSG single-machine infinite-bus system is shown in Formula (10).

$$\begin{cases} S_+ = \int_{\delta_0}^{\delta_c} (P_{\text{ref}} - P_{\text{ef}} - D\omega_0 \Delta\omega) d\delta^{1-\lambda} \\ S_- = \int_{\delta_c}^{\delta_1} (P_{\text{en}} - P_{\text{ref}} + D\omega_0 \Delta\omega) d\delta^{1-\lambda} \end{cases} \quad (10)$$

Given that the fractional integral order λ is less than one, the power angle characteristic curve will undergo a transformation. In comparison to the conventional VSG control strategy, the fractional-order VSG control strategy enhances the power angle characteristic curve and diminishes the acceleration area in the event of a fault. Once the fault has been rectified, the deceleration area is increased and the transient stability of the system is enhanced.

III. SIMULATION ANALYSIS

In order to ascertain the viability and superiority of the control strategy proposed in this paper, the VSG grid-connected circuit and control model depicted in Figure 1 are constructed within the MATLAB/Simulink environment. The principal parameters of the circuit and controller are presented in Fig. 1.

TABLE I. VSG GRID-CONNECTED PARAMETERS

Parameters	Numerical
Dc power supply U_{dc}/V	800
Rated Frequency f/Hz	50

The VSG parallel power supply system initiates a steady state operation, and a three-phase ground short-circuit fault is observed at the load bus at 2s. The grid-side voltage drop is 0.24 p.u., and the fault is removed at 2.1975 s. The time required for the system power angle to restore stability under different working conditions is analysed under the same fault removal

TABLE II. THE VOLTAGE DROPS TO 0.24P.U.

Variables	J	D	λ
Covsg	50	1000	\
Fovsg1	50	1000	0.25
Fovsg2	50	1000	0.5

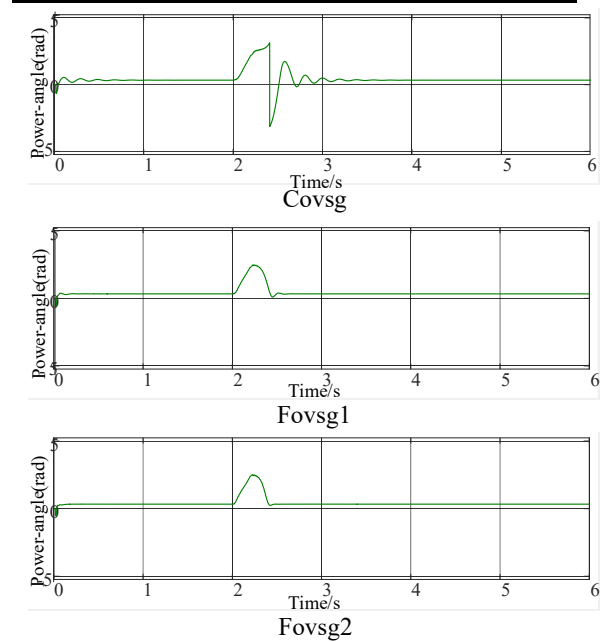


Fig. 7. Comparison of system power angle stability waveforms

Fig. 7. illustrates that the power angle stability recovery of the traditional VSG control strategy is the slowest. Following a series of oscillations, the power angle achieves stability at 3.57 seconds. The fractional-order VSG control strategy is employed. When $\lambda = 0.25$, the power angle reaches a stable state in 2.57 seconds, which is 1 second faster than the traditional VSG control strategy. When $\lambda = 0.5$, the time required for the power angle to reach a stable state is 2.43 seconds, which is 1.14 seconds faster than the traditional VSG control strategy. The

fractional-order VSG control strategy is therefore adopted. In comparison to the traditional VSG control strategy, the stable recovery speed of the power angle is observed to be faster.

IV. CONCLUSION

This paper addresses the challenge of conducting a transient synchronous stability analysis of a VSG island parallel system in accordance with the traditional equal area rule. To address this challenge, the paper proposes an equal area rule that considers fractional order. The incorporation of a fractional order integral order $\lambda < 1$ of the acceleration and deceleration area of the fractional order VSG single machine infinite bus system results in an increase in the power angle characteristic curve. Consequently, in the event of a system failure, the acceleration area is diminished while the deceleration area is augmented, thereby enhancing the transient stability of the system. The simulation results corroborate the accuracy of the proposed method. The simulation results demonstrate that, when considering both the transient stability of the system and the time required for system adjustment following the removal of a fault, a reduction in the fractional order of the inertial link results in enhanced transient stability and a more rapid recovery in power angle. The implementation of a fractional-order VSG control strategy within a grid-connected microgrid inverter facilitates an enhancement in the transient stability performance of the system, thereby ensuring a more stable operational profile in the event of a fault.

REFERENCES

- [1] KONG Xiangping, FENG Chang, DING Hao, et al. Application prospective and development trends of virtual generator technology[J]. Electric Power Engineering Technology, 2017, 36(5): 35-44.
- [2] LI Dongdong, SUN Yaru, XU Bo, et al. Minimum inertia and primary frequency capacity assessment for a new energy high permeability power system considering frequency stability[J]. Power System Protection and Control, 2021, 49(23): 54-61.
- [3] CHENG Cheng, XIE Shaojun, TAN Lingjuan, et al. Nonlinear model and stability analysis method for grid-following inverter[J]. Automation of Electric Power Systems, 2022, 46(6): 137-143..
- [4] WANG Guodong, LI Haiyang. Accurate control of reactive power of grid-forming inverters based on impedance matching[J]. Power Electronics, 2022, 56(6): 45-48.
- [5] CHAIBI Y, ALLOUHI A, SALHI M, et al. Annual performance analysis of different maximum power point tracking techniques used in photovoltaic systems[J]. Protection and Control of Modern Power Systems, 2019, 4(2): 171-180.
- [6] LÜ Zhipeng, SHENG Wanxing, LIU Haitao, et al. Application and challenge of virtual synchronous machine technology in power system[J]. Proceedings of the CSEE, 2017, 37(2): 349-360.
- [7] ZHANG Chenyu, YANG Yun, YUAN Xiaodong, et al. Modeling method of virtual synchronous machine considering damping and inertia[J]. Electric Power Engineering Technology, 2018, 37(5): 45-49. ZHU Xiaorong, LU Guowei, XIE Wanying. Robust planning of energy storage in distribution network considering sourcenetwork-load flexible resources [J] . Electric Power Automation Equipment, 2021, 41 (8) : 8 - 16, 40.
- [8] Mao F B, Zhang X, Liu F, et al. Research on 468 improved VSG control strategy based on virtual damping compensation[J]. Power Electronics, 2016, 50(9): 75-78.
- [9] N Liu Y, Chen J F, Hou X C, et al. Dynamic frequency stability control strategy of microgrid based on adaptive virtual inertia[J]. Automation of Electric Power Systems, 2018, 42(9): 75-82.
- [10] Li D D, Zhu Q W, Cheng Y Z, et al. Control strategy of virtual synchronous generator based on adaptive inertia damping integrated control algorithm[J]. Electric Power Automation Equipment, 2017, 37(11): 72-77.
- [11] Li P. Research on adaptive sliding mode control strategy under micro-grid virtual synchronous generator[D]. Chengdu: School of Electrical Engineering, Southwest Jiaotong University, 2017: 1-75.
- [12] Qu Z S, Cai Y Y, Yang H, et al. Power decoupling control strategy of virtual synchronizer based on adaptive virtual impedance[J]. Automation of Electric Power Systems, 2018, 42(17): 58-72.
- [13] Du Y, Su J H, Zhang L C, et al. A mode adaptive micro-frequency frequency modulation control method[J]. Proceedings of the CSEE, 2013, 33(19): 67-75.
- [14] Xu H Z, Zhang X, Liu F, et al. VSG control strategy based on virtual inertia of lead lag phase[J]. Proceedings of the CSEE, 2017, 37(7): 1918-1926.
- [15] Xue D Y. Fractional calculus and fractional order control[M]. Beijing: Science Press, 2018: 1-226.
- [16] Qi Z D, Zhou X, Bian H J, et al. PEMFC dynamic modeling and fuzzy fractional order PI λ Du control[J]. Control and Decision, 2017, 32(6): 1148-1152.
- [17] Yang B, Shu H C, Zhu D N, et al. Optimal passive fractional-order PID control of photovoltaic inverter based on group grey wolf optimization[J]. Control and Decision, 2020, 35(3): 593-603
- [18] Y. Yu, Y. Guan, W. Kang, S. K. Chaudhary, J. C. Vasquez and J. M. Guerrero, "Fractional-Order Virtual Synchronous Generator," in IEEE Transactions on Power Electronics, vol. 38, no. 6, pp. 6874-6879, June 2023.
- [19] Zhang Y N, Zhou X M. Virtual synchronous generator control technology with fractional virtual inertia for grid-connected inverters[J]. Control and Decision, 2021, 36(02):463-468.